



LNF-03/008(R)
6 Maggio 2003

**AN X-BAND STRUCTURE FOR A LONGITUDINAL EMITTANCE
CORRECTION AT SPARC**

A.Bacci¹, M.Migliorati², L.Palumbo² and B.Spataro³

(1) INFN-LASA di Milano – Via Fratelli Cervi 201- 20090 Segrate (MI)

*(2) INFN-LNF and Università' di Roma "La Sapienza", Dip. Energetica-Via A. Scarpa 14,00161
Roma*

(3) INFN-LNF, Via E.Fermi 40,00044 Frascati (RM)

Abstract

The paper presents the design of a compact standing wave accelerating structure operating at a frequency $f = 11.424$ GHz for the low energy part of the X-FEL project to be realized at the Frascati Laboratories (SPARC). The structure, designed for obtaining a 5 MeV energy gain, has to be used for linearizing the longitudinal space phase in the Frascati Linac Coherent Light Source. Numerical electromagnetic simulations were carried out by using the numerical codes SUPERFISH and OSCARD2D in the frequency domain and ABCI in the time domain.

This report describes the detailed behaviour of main RF parameters of a standing wave accelerating structure operating on π mode.

INTRODUCTION

A possible schematic layout to be used for enhancing the bunch compression performances for the X-FEL project to be constructed at the Frascati Laboratories is reported in Fig. 1.

It is mainly constituted by a photo-cathode RF gun which works in the S-Band at a frequency $F=2.856$ GHz and deliveries bunches with a 5 MeV kinetic energy, 1 nC charge and 10 psec bunch length; an X-Band accelerating structure with frequency equal to the fourth harmonic of the S-Band frequency; a travelling wave velocity buncher which works at a frequency $F=2.856$ GHz ; two $2\pi/3$ travelling wave constant gradient structures operating at $F=2.856$ GHz.

For compensating the non-linearity distortions due to the RF curvature of the 2.856 GHz accelerating cavities, the use of a short higher harmonic standing wave accelerating structures operating at 11.424 GHz is required.

The analysis of the combined action of the X-Band accelerator and the bunch compressor on the beam transport is under study. Since only the single bunch operation is foreseen, the beam dynamics is not affected by the long range wake-fields, as a consequence no dedicated dampers of the parasitic higher order modes are adopted of the section X-Band.

The advantages of using X-Band electron accelerating structures are well known: smaller size, higher shunt impedance, higher breakdown threshold level and short filling time.

The technologies in S-Band frequency range are readily available at this frequency range since they have been widely tested in many scientific and industrial applications.

The technologies in the X-Band accelerating structures, high power sources and modulators have been also developed at KEK^{1,2}, SLAC^{3,4,5} and Varian^{6,7} for the future linear colliders.

In order to obtain the longitudinal phase space linearization and from beam dynamics considerations, we are going to design a compact 5 MeV X-Band accelerating section with field uniformity on the longitudinal axis and a 4 mm beam tube radius.

For proper beam dynamics, field amplitude and phase along the accelerator structure must be kept constant. The RF stability problems influence the beam dynamics design too, because the length and the frequency of the structure are no longer free parameters.

RF stability during operation and tuning tolerances are crucial points for the RF structure design in the high frequency range. The complexity of machining, tight mechanical tolerances and alignments, are therefore important aspects which have to be taken into account in the design activity.

This report is devoted to the choice of the fundamental RF parameters as the form factor R_{sh}/Q , quality factor Q , power losses, field profiles, dispersion curves, cooling system, electric field breakdown of a standing wave structure operating on π mode.

CHOICE OF THE ACCELERATING STRUCTURE TYPE

The design of the particle accelerators of new generation is defined on the basis of a compromise among several factors: RF parameters, beam dynamics, RF power sources, easy fabrication, small sensitivity to construction errors, economical reasons and so on.

In order to minimize the input power requirements for a given accelerating gradient, the RF accelerating structures have to be designed with the aim of maximizing the shunt impedance. On the other hand, the accelerating section performances could be limited by effects such as the beam loading, instabilities, beam break-up etc., caused by the interaction between the beam and the sections.

As an example, a figure of merit for the accelerating structure is the efficiency with which it converts average input electromagnetic energy per unit length, into average accelerating gradient. Then, if P_b is the average beam power and P_{rf} the average RF power fed into the structure, the small fraction of energy extracted by beam defined as $\epsilon = P_b / P_{rf}$ has to be kept around to some per cent for getting a satisfactory energy spread.

On the basis of these simple considerations, the global RF properties for designing the accelerating structure are therefore summarized in the following⁷:

- 1) High accelerating field gradient to reduce the accelerator length;
- 2) High shunt impedance to reduce the requirement of RF power;
- 3) Low ratios E_p/E_0 and B_p/E_0 , where E_p and B_p are the surface electric and magnetic peak fields respectively and E_0 is the average accelerating field, to minimize dark currents, to achieve the highest possible field gradient before reaching the break down condition and to reduce thermal effects.
- 4) High ratio E_0/W where W is the energy stored in the structure per unit length that is a measure of the efficiency with which the available energy is used for the operating mode;
- 5) High group velocity in order to reduce the filling time of the section and therefore to realize a section less sensitive to the mechanical imperfections;
- 6) Low content of longitudinal and transverse higher order modes which can be excited by the bunches traversing the structure and those can affect the beam dynamics;
- 7) appropriate shape profile for avoiding the generation of multipactoring phenomena which could limit the accelerating section performances.

Our main concern is to construct an accelerating structure with the requirements reported below

- 1) average accelerating voltage, $V = 5 \text{ MV}$;
- 2) compact axial length, $L = 12 \text{ cm}$;
- 3) beam aperture diameter, $\phi = 8 \text{ mm}$;
- 4) operating frequency, $F = 11.424 \text{ GHz}$;
- 5) ratio phase to light velocity, $v_\phi / c = 1$
- 6) pulse charge, $Q = 1 \text{ nC}$;
- 7) full pulse length, $l_\tau = 10 \text{ psec}$ (much shorter than one filling time of the accelerating section);
- 8) single pulse operation;
- 9) pulse repetition rate frequency, $f = 50 \text{ Hz}$.

In the realization of an accelerating structure it is relevant to know the sensitivity of field amplitudes to errors in tuning, to unwanted perturbations or to the presence of tuners. This subject has been already treated by the application of the perturbation theory to the equivalent circuit representation⁸ or by considering the multiple reflection of a wave traveling on a finite chain of coupled resonators⁹ and including also the presence of the beam loading¹⁰.

The standing wave operation on the π mode has the highest shunt impedance but it has the disadvantage of being sensitive to the beam loading and detuning effects; the $\pi/2$ mode has the advantage of being less sensitive to beam loading and detuning effects, but has the disadvantage of having a shunt impedance half than the π mode.

A combined π and $\pi/2$ mode structure with multi-periodicity or bi-periodic $\pi/2$ mode, is surely of interest but it is more expensive and difficult to realize.

In case of the accelerating sections made-up by many coupling cells where the mechanical tolerances accuracy is more rigid, the choice of the section bi-periodic $\pi/2$ mode is particularly

attractive since it gives rise to a good field stability against unwanted perturbations, or introduced by tuners, machining errors and tighter mechanical tolerances, even though it gives a shunt impedance slightly smaller than the π mode. Since we want to get a shunt impedance as high as possible and use a section formed by a limited coupling cavity number, we decided to work on the π mode standing wave configuration. Moreover, no specific effect due to the beam loading and beam dynamics has to be expected since the operation with a small average current and single bunch is adopted.

The fourth harmonic frequency of the main Linac one implies small physical dimensions and thereby the dissipated power constitutes one of the main constraints, as well.

A reasonable upper limit on the average power dissipation has been estimated to be around at 4 kW/m. By assuming a 3 MW input peak power with a duty cycle of 10^{-4} , for determining a 5 MV average accelerating voltage (or 42 MV/m average accelerating gradient), a minimum of 8 M Ω shunt impedance with a 2.5 kW/m dissipated power have been estimated. Operation with rather high quality factor Q is also required for preventing the excitation of neighboring modes.

To meet the full requirements by keeping a flexibility margin, a section with simpler geometry which is cheap and of reliable construction and with satisfactory mechanical tolerances has been chosen.

The structure consists of a series of 9 cylindrical profile resonators with identical coupling cells operating on π mode by forcing the cavities periodicity at $p=1 = \beta\lambda / 2 = 1.312$ cm and assuming relativistic particles. Calculations were carried out for a 2 and 3 mm thickness iris in order to estimate the structure stability. The detailed RF properties and the thermal behaviour of the π mode are described later in the following subsections.

ACCELERATING STRUCTURE RF PROPERTIES

The longitudinal available space, the minimum beam aperture and the operating frequency dictated the physical dimensions of the structure. The frequency analysis was performed by using the SUPERFISH¹¹ and OSCAR2D¹² computation codes.

Simulations were carried out with a half, whole and two cells geometries, by using smaller meshes, about 0.01cm and 0.005cm, by the order of magnitude with respect to the achievable minimum mechanical tolerances, to reduce the computation effort, to determine a higher accuracy of the results and to confirm the main RF parameters behaviour trend.

The comparison of the results gave accurate information on the section stability in term of shunt impedance and frequency sensitivity as function of the cavity sizes.

The form factor $R/(Q*L)$ per unit length and the merit factor Q have been calculated as a function of the iris radius. To do that every time the cavity sizes were re-adjusted to keep the cavity resonating at the nominal frequency $f = 11.424$ GHz. Since the beam aperture requirement is quite large we could not push the shunt impedance to a very high value.

As a conclusion, for a 1.054 cm cavity radius, 2 mm iris thickness and 4 mm iris radius, about 80 M Ω /m are obtained, while the rates of change of resonance frequency as function of cavity and iris radius have been estimated to be around $\Delta f = 12$ MHz/10 μ m and $\Delta f = 4$ MHz/10 μ m, respectively.

a) accelerating structure dispersion curve calculations

The final investigated section, constituted by 9 cylindrical cavities resonator which fulfil the design requirements is shown in Fig. 2a.

To get a better understanding of RF behaviour of the section, the oscillating modes distributed along the dispersion curve were calculated and presented in the Fig.2b. In order to obtain the theoretical dispersion relation behaviour, symmetry planes located at the centre of the end-cells with different combinations of electric and magnetic mirror boundary conditions have been simulated. The shape of the dispersion curve is defined by two frequencies f_0 and f_π corresponding to the modes 0 and π . Then, for obtaining the final dispersion curve, a structure with full end-cells with coupling tubes was examined.

A comparison between the numerical results and an analytical expression of the dispersion curve has also been used^{13,14}:

$$\omega_\phi^2 = \omega_0^2 + 0.5 \cdot (\omega_\pi^2 - \omega_0^2) \cdot (1 - \cos\phi) \quad 1$$

The global analysis is reported in Fig.2b where the points denote the resonance frequencies of the individual modes and the solid line is the fit calculated with the analytical expression.

It is relevant to remark the excellent agreement between the theoretical model and the numerical simulations. Moreover, due to the fact that a real structure has evanescent fields inside the coupling tubes, the individual modes change their frequencies¹⁵ but the fit of the two examined cases remains substantially unchanged.

The separation of the lower and upper cut-off frequencies allows to determine the bandwidth of the structure.

The coupling coefficient given^{14,15,16}:

$$K = (\omega_\pi - \omega_0) / \omega_{\pi/2}$$

has been estimated to be about $K = 2.42 \%$. A check has been also performed by using the theory :

$$K = \frac{\omega_\pi - \omega_0}{\omega_{\pi/2}} \approx k e^{-\alpha h}$$

with

3

$$k \equiv \frac{4a^3}{3\pi J_1^2(2.405)b^2 l} \ll 1 \quad \text{and} \quad \alpha = \sqrt{\left(\frac{2.405}{a}\right)^2 - \frac{\omega^2}{c^2}}$$

with a the iris radius, b the cavity radius, l the axial length of the cavity, α the attenuation per unit length of the field and h the iris thickness.

By substituting the corresponding values derived from Fig. 2, the fractional bandwidth of the TM_{010} pass-band is evaluated to be $K=2.27 \%$, about a 6% less of the previous one.

The theoretical model underestimates the coupling coefficient since it takes into account a hard edge of the iris region against the rounded shape of the real structure. In any case, we retain that the comparison between the numerical and theoretical results are in an excellent agreement.

In order to predict the mode resonances overlapping behavior, the spacing frequency between the operating mode and the adjacent one has been evaluated. It gives a $\Delta f = 9$ MHz frequency separation, about 7 times the unloaded operating mode bandwidth.

In order to check the validity of the results, a similar structure with a 3 mm thickness iris, 1.0595 cm radius and the previous periodicity, gave a $\Delta f = 6.3$ MHz frequencies separation, which is considerable lower than the first one.

In addition, the coupling coefficient calculated with the numerical analysis is estimated to be $K = 1.76\%$, while the one estimated with analytical model gives a lower value ($K = 1.4\%$).

It is interesting to remark that with higher h , a value of K 33 % smaller than the numerical one is obtained because of a greater attenuation introduced by the hard edge shape effect of the irises, as it is demanded by the theoretical model approximation.

In Fig. 3. the dispersion curve for a 3 mm thickness irises and the geometry sizes are illustrated, while in Fig. 4 the dispersion curves for both 2 and 3 mm thickness are reported in the same picture for comparison.

In conclusion, we believe that the structure with a 2 mm thickness is surely better performing.

b) working mode

The average accelerating voltage for the described design is imposed to be 5 MV voltage due to the relatively low operating energy and it has to be achieved with a field flatness on the longitudinal axis. On the other hand, as it is above mentioned, one of the basic requirements of the section is the power dissipation.

In Fig. 5 we show the field distribution profile of the accelerating mode of the finite multi-cell standing wave structure with beam tubes obtained by keeping the same cavities radius. By the inspection of the figure, the field flatness is clearly not achieved. For sake of completeness, it is evident that the peak in the end-cells is about 1/3 with respect to that of the central cavity.

In order to get the field compensation on the longitudinal axis the procedure reported by other authors is followed¹⁴. As a consequence, the end-cells have to be engineered with a lower different radius (of the order of 40 μm) for obtaining a π mode field flatness on axis as it is shown in Fig. 6.

By considering a safety margin, we obtained a shunt impedance per unit length, which measures the accelerating quality of the section, equal to $R_{\text{sh}} = 77 \text{ M}\Omega/\text{m}$. It gives a satisfactory average power loss around 300 W by assuming an operation with a 10^{-4} duty cycle.

Peak electric surface field is a factor 6 below with respect to that measured at SLAC⁷. In addition, the estimate of the energy spread due to beam loading was calculated with the analytical expression^{17,18} :

$$\epsilon = \frac{bNe\omega}{E_0} \cdot \frac{R_{\text{sh}}}{Q} \quad 4$$

where bN is the number of particles per beam pulse (consisting of b closely spaced bunches), e is the elementary charge, $\omega/2\pi$ the RF frequency, E_0 the average accelerating gradient and R_{sh}/Q the form factor per unit length.

Taking $R_{\text{sh}}/Q = 9161 \text{ }\Omega/\text{m}$, $N = 6.24 \cdot 10^9$ particles, $E_0 = 42 \text{ MV/m}$ and $F = 11.424 \text{ GHz}$, the energy spread is evaluated to be $\pm 0.78\%$.

By using the ABCI^{19,20} computer program the global losses of the structure were estimated, as well. The computation code solves the Maxwell equations directly in time domain when a bunched beam passes through an axi-symmetric section.

The total energy losses is calculated with $\Delta E = -K_1 q^2$ where q is the beam charge and K_1 the longitudinal loss parameter.

The longitudinal loss parameter depends on the structure shape and calculated as the longitudinal wake potential convolution over particle distribution. The simulations carried out with $\sigma = 1 \text{ mm}$ and by assuming a Gaussian distribution, gave about $\Delta E = 37 \text{ keV}$.

In Tab.1 the losses contribution due to the longitudinal higher order modes is also shown.

The performance of the accelerating structure may also be limited by the resonant electron discharges or “multipactoring”.

It is well known that for reducing or eliminating this phenomenon it is recommended to have a curved profile for the resonator surfaces or to use asymmetric cavity shapes^{21,22}.

In the described design for the above reasons a compact size standard geometry has been chosen, making the manufacturing easier and cheaper. Here some considerations on “multipactoring” have to be explained.

Due to the big aperture of the structure, we believe that the “two points multipactoring” in the gap region of the cavity is unlikely to occur since the counteraction of the radial electric force and magnetic force is uncompensated, thereby no resonant discharges have to be determined. According to our experience, the “one point multipactoring” can happen at some lower fields levels. Moreover, a two points special kind “multipactoring”²³ “ could happen in some levels of the operating condition, as well.

We believe that the presence of non-resonant electron loading or dark current gives no specific trouble since the estimate of the average accelerating electric field is a by 30% lower than the minimum threshold field limit²⁴. The “multipactoring” study will be analyzed in details in a forthcoming paper.

The complete study of the accelerating section was also performed with 3 mm thickness iris by keeping unchanged the periodicity of the structure.

From the Table 1, even though similar results have been obtained, because of a lower quality factor Q and a smaller spacing frequencies between the working mode and the adjacent one, we decided to make a choice for a structure with 2 mm of thickness iris.

THERMAL ANALYSIS

A rise in temperature will vary the accelerator dimensions and the frequency characteristic will change accordingly. The temperature rise can be reduced by means of a cooling system. For getting the frequency variation behavior as a function of the temperature change the thermal study is also required.

We wish to estimate the frequency change caused by a change in temperature over the accelerating structure operating on π mode. We will assume that a closed cooling water system is used in order to keep the operating temperature at 40 °C.

A preliminary thermal analysis of the structure has been determined by means of the ANSYS²⁵ software. Fig. 7 depicts the thermal flux on an important region of the boundary's structure and the distributed temperature inside the metal, by assuming to use copper.

The frequency shift behavior versus the heating of the structure has been studied by the ANSYS and SUPER-FISH. It is shown that a temperature variation of $\Delta T=1^\circ\text{C}$ causes a 180 kHz frequency shift by assuming an isotropic expansion and 60 kHz frequency shift related to the power distribution shown in the Fig. 7.

It means that a 0.1 °C temperature stabilization can be applied for controlling the structure frequency. Additional checks on this topics are in progress, and more detailed studies will be examined and described in a forthcoming paper.

SUMMARY AND ACTION

We have chosen an X-band accelerating structure operating on π mode as possible candidate for the fourth harmonic standing wave section. The choice is dictated, mainly, by higher shunt impedance of the π mode structure with respect to that operating on $\pi/2$ mode. Even though the $\pi/2$

mode has the advantage of being less sensitive to beam loading and detuning, these effects do not seem to be critical for π mode structure since it consists of a limited number of cavities and operates with a small average current in single bunch regime.

A combined π and $\pi/2$ mode structure with multi-periodicity or bi-periodic $\pi/2$ mode, is surely of interest, but it is more expensive and difficult to realize.

By comparing π mode structures with iris thickness of 2 mm and 3 mm, we decided to work with thinner irises due to higher separation between accelerating mode and adjacent one.

A complete electromagnetic characterization of the section has been carried out with numerical codes SUPERFISH, OSCAR2D and ABCI and the main RF parameters are summarized in Table 1. In addition thermal analysis has been by showing 0.1°C necessary to stabilize the structure.

The design presented here should use therefore the technology experienced from the recent developments to produce a practical and economical realization of the section.

A prototype is under construction and tests at low power are foreseen, too. The detailed analysis of a bi-periodic section will be presented in a forthcoming paper.

ACKNOWLEDGEMENTS

Useful discussion with Dr. D. Alesini, V. Fusco, A. Mostacci and R. Parodi are gratefully acknowledged.

REFERENCES

- 1) S. Takeda et al., Particle Accelerator,30 (1990),1101.
- 2) K. Takata, Proc. First Workshop on Japan Linear Collider (JLC),KEK, Oct. 24-25, 1989, 2.
- 3) J.W. Wang and G.A. Loew,"Measurements of ultimate Accelerating Gradients in the SLAC Disk-loaded Structure," 1985 PAC, Vancouver, B.C., May 1985, SLAC-PUB-3597, March 1985.
- 4) J. W.Wang, V. Nguyen-Tuong and G.A. Loew, " RF Breakdown Studies in a SLAC Disk-loaded Structure," Proceedings of the 1986 Linear Accelerator Conference, Stanford, Ca, June 1986, SLAC-PUB-3940, April 1986.
- 5) J. W. Wang and G.A. Loew,"Progress Report on New RF Breakdown Studies in an S-band Structure at SLAC,"presented at the 1987 PAC,Washington,D.C.,March 1987, SLAC-PUB-4247,February 1987.
- 6) E. Tanabe,J. W. Wang and G.A. Loew, "Voltage Breakdown at X-band and C-band Frequencies," Proceedings of the 1986 Linear Accelerator Conference, Stanford, Ca, June 1986.
- 7) J. W. Wang,"RF Properties of Periodic Accelerating structures for Linear Colliders", SLAC-Report-339, July 1989.
- 8) J. R. Rees, "A Perturbation Approach to Calculating the behavior of Multi-cell Radiofrequency Accelerating Structures" PEP-255, Stanford Linear Accelerator Centre (1976).
- 9) P. B. Wilson, IEEE Trans. Nucl. Sci. NS-16, No. 3, 1092 (1969).
- 10) T. Nishikava,IEEE Trans. On Nuc. Sci., NS-12 n. 3, 630 (1965).
- 11) Poisson Superfish, James H. Billen and Lloyd M. Young, software produced under U.S. Government by Los Alamos National Laboratory, Particle Accelerators 7 (4), 213-222 (1976).
- 12) P. Fernandes and R. Parodi," LALAGE – A Computer Program to Calculate the TM Modes of Cylindrically Symmetrical Multicell Resonant Structures",PAC 1982,Vol. 12, pp. 131-137.
- 13) S. Kulinski et al." Linac for Afrodite, Solution with Pulse Compression",Memo AF-13,Frascati 30 October,1986.
- 14) P. Fernandes and R.Parodi,"On Compensation of Field Unflatness of Axial Electric Field in Multi-cell Resonant Structures",Particle Acceleratos 14,(1984).
- 15) H.Padamsee, J.Knobloch,T.Hays, "RF Superconductivity for Accelerators", John Wiley & Sons, (pages 131-133).
- 16) Thomas P.Wangler"Principles of RF Linear Accelerators" John Wiley & Sons (pages 76-77).
- 17) W. Schnell,"Dissipation Versus Peak Power in a Classical Linac", LEP-RF/WS/ps, CLIC note 4, 22nd October 1985.
- 18) P. Brunet:"Section Accelateur Fort Courant en Ondes Stationnaires", LAL/PI/80-20,Orsay May 1980.
- 19) Y.H. Chin, CERN LEP-TH/88-3, 1988.
- 20) Y.H. Chin, "Advances and Applications of ABCI", 1993 PAC Washington D.C., May 17-20, 1993.
- 21) R.Boni,V.,Chimenti,P. Fernandes,R. Parodi, B.Spataro,F.Tazzioli," Design and Operation of a Multipacting-Free 51.4 MHz Rf Accelerating Cavity", NIM A274(1989),49-55.

- 22) B.Spataro, R Boni, "The Multipactorin-Free RF Cavity of the DAΦNE Accumulator", INFN-LNF-DAΦNE-Technical-Note, Note:RF-Frascati,July16,1996.
- 23) P.Fabbricatore, G.Gemme, R.Musenich, R.Parodi, S.Pittaluga, "Discharge in spherical cavity at 3GHz",VII Workshop on RF Superconducting October 17-20, 1995, Vol.2, pag. 385.
- 24) G. Bienvenu,P. Fernandes and R. Parodi,"An Investigation on the Field Emitted Electrons in Ttraveling Wave Accelerating Structure",NIM A320(1992)1-8.
- 25) ANSYS is a simulation software used to determine real-world structural, thermal electromagnetic and fluid-flow behavior of 3-D product designs. www.ansys.com

Table 1

STANDING WAVE X BAND ACCELERATING STRUCTURE – RF PARAMETERS LIST
CALCULATED BY USING SUPERFISH AND OSCAR2D CODES

	π mode	π mode
-Frequency, F (MHz)	11426*	11427*
-Length for calculation, L (cm)	11.81	11.81
-Beam tube length, l (cm)	3	3
-Cavity number, n_b	9	9
-Ratio of phase to light velocity, v_ϕ/c	1	1
-Structure periodicity, L_p (cm)	1.3121	1.3121
-Beam hole radius, r (cm)	0.4	0.4
-Iris Thickness, t(cm)	0.3	0.2
-Transit time factor, T	0.739	0.731
-Factor of merit, Q	8069.46	8413.18
-Form factor, R_{sh}/Q (Ω/m)	9232.34	9165.38
-Shunt impedance, R_{sh} ($M\Omega/m$)	74.5	77.11
- Coupling coefficient, K(%)	1.76	2.42
-Peak power, P (MW)	2.795	2.701
-Energy stored in cavity of length L, W (joules)	0.314	0.316
-Peak power per meter, P/m (MW/m)	23.66	22.87
-Energy stored in cavity per meter, W/m (joules/m)	2.659	2.677
-Duty cycle, D.C.	10^{-4}	10^{-4}
-Repetition frequency, f (Hz)	50	50
-Power dissipation, P_d (Watt)	279.5	270.1
-Average accelerating field, E_{acc} (MV/m)	42	42
-Peak axial electric field, E_{max} (MV/m)	56.84	57.49
-Kilpatrick factor	1.089	1.197
-Peak surface electric field, E_{sur} (MV/m)	95.36	104.84
-Ratio of peak to average fields E_{max}/E_{acc}	1.35	1.37
-Ratio of peak to average fields E_{sur}/E_{acc}	2.27	2.496
-Ratio of peak fields B_{max}/E_{sur} (mT/MV/m)	1.89	1.65
-Pulse charge, C (nC)	1	1
-Pulse length, τ (psec)	10	10
- Number of bunches, n	1	1
-Average beam power, P_{baver} (W)	0.248	0.248
-Energy spread due to the beam loading, %	± 0.788	± 0.783
-Loss parameters due to the HOM's K_p (V/pC)	17.77	16.95
-Loss parameter of the operating mode, K_0 (V/pC)	19.57	19.43

* Mesh 0.03 cm. With a mesh of 0.01 cm, we have too long calculation time, but we have seen that the frequency value converge to 11424 MHz.

Figures caption

Fig. 1 Lay-out of the first part of the X-FEL project. It is possible to see the X-band structure is useful to correct locally the RF curvature and to avoid the increase of the longitudinal emittance which limits the current.

Figs. 2a Shape and size of the simulated structures. **2b** Dispersions curve of the structures. The squares denote the resonance frequencies of the individual modes for a structure with coupling tube, the points denote the modes for a structure closed with metal mirrors and the solid line is a fit that arises from the analytic expression.

Fig. 3 It is the same of the figure 2, but for a 3 mm iris thickness structure.

Fig. 4 Superposition of Fig. 2 and Fig. 3. It show the important difference in the separation of the modes, for the two different structures.

Fig. 5 Electric field profile of the accelerating mode in a structure with beam-tube and with a constant cavity radius.

Fig. 6 Electric field profile of the accelerating mode in a structure with beam-tube and with the end-cells engineered with a different radius in order to obtain a flat π -mode (field amplitude equal in all N cells).

Fig. 7 Thermal flux on an important region of boundary's structure and the distributed temperature inside the metal (copper). Study performed with ANSYS.

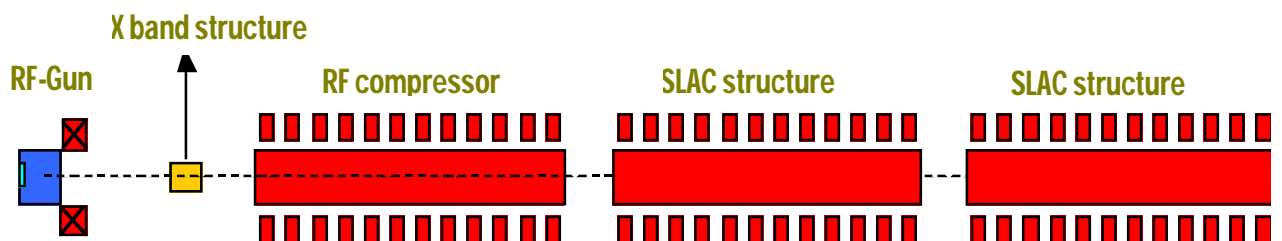
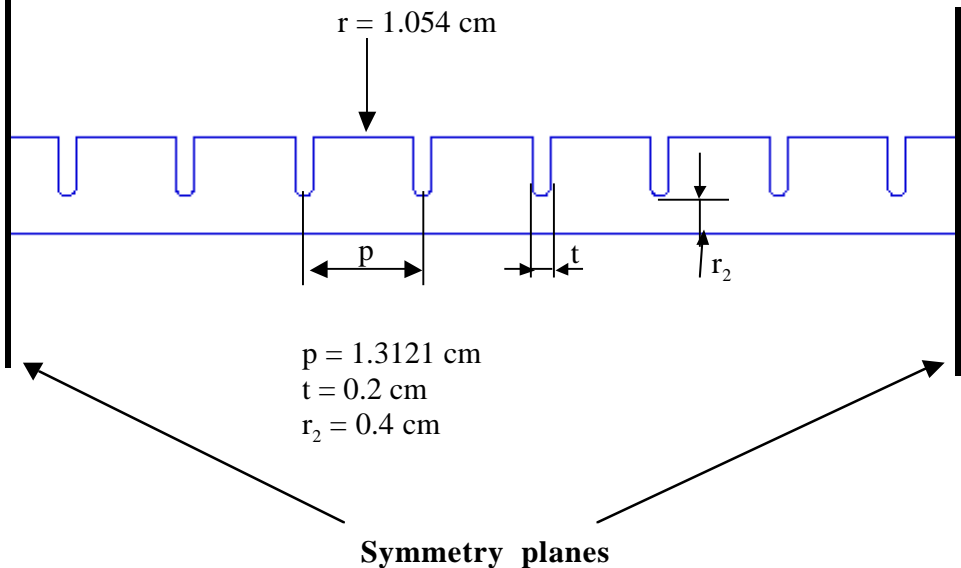


Fig. 1

Simulated structure with no coupling tubes



Simulated structure with coupling

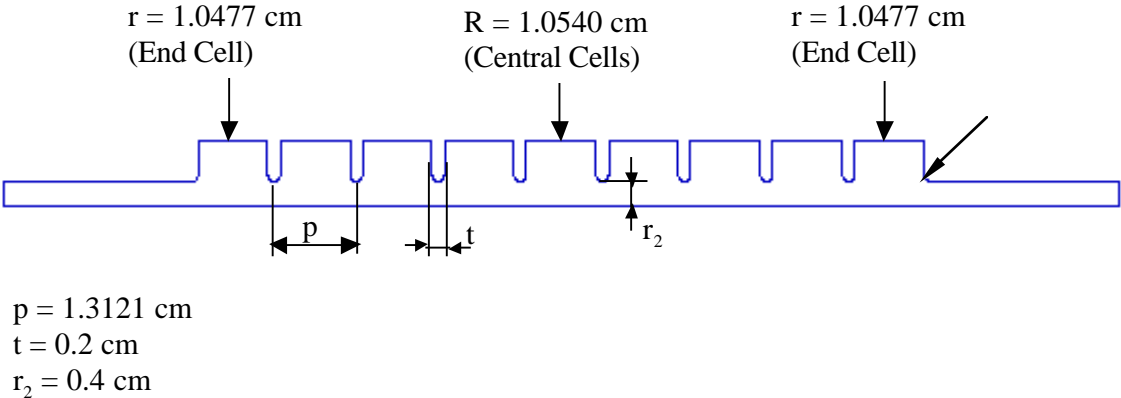
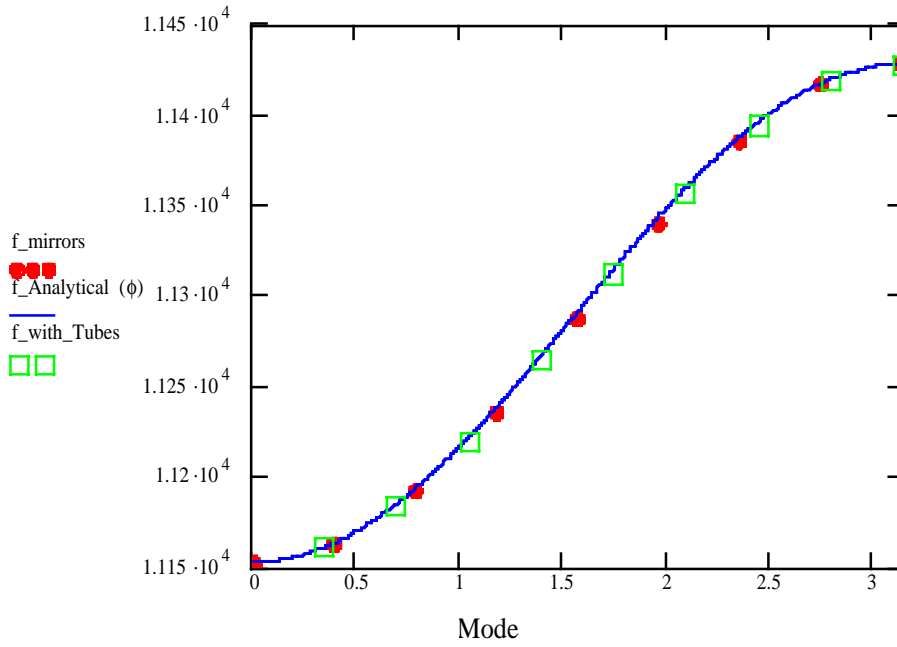
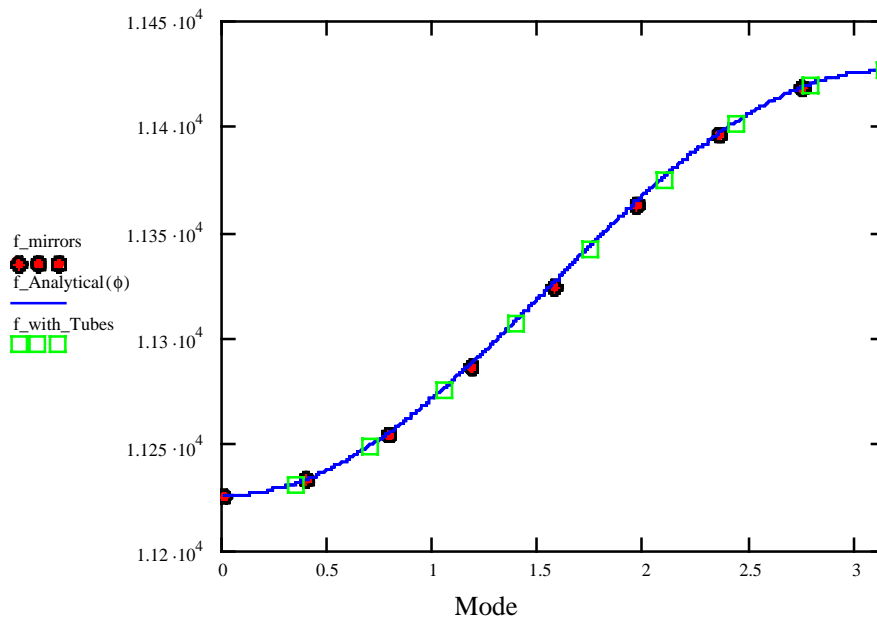


Fig. 2a



structure with mirrors		structure with tubes	
Frequency [MHz]	Mode [π]	Frequency [MHz]	Mode [π]
11152.818	0	11160.784	1/9
11162.906	1/8	11183.868	2/9
11191.717	1/4	11219.481	1/3
11235.333	3/8	11263.701	4/9
11287.522	1/2	11311.225	5/9
11340.448	5/8	11356.593	2/3
11386.000	3/4	11393.989	7/9
11416.834	7/8	11418.634	8/9
11427.704	1	11427.465	1

Fig. 2b



structure with mirrors

Frequency [MHz]	Mode [π]
11226.065	0
11233.518	1/8
11254.808	1/4
11286.885	3/8
11324.981	1/2
11363.477	5/8
11396.442	3/4
11418.442	7/8
11426.240	1

structure with tubes

Frequency [MHz]	Mode [π]
11231.958	1/9
11248.970	2/9
11275.146	1/3
11307.483	4/9
11342.200	5/9
11375.053	2/3
11402.022	7/9
11419.735	8/9
11426.078	1

Structure with mirrors sizes:

Cells radius 1.0595 cm
 Iris thickness 0.3 cm
 Beam hole radius 0.4 cm

Structure with coupling tubes sizes:

Central cells radius 1.0595 cm
 End-cells radius 1.0550 cm
 Iris thickness 0.3 cm
 Beam hole radius 0.4 cm

Fig. 3

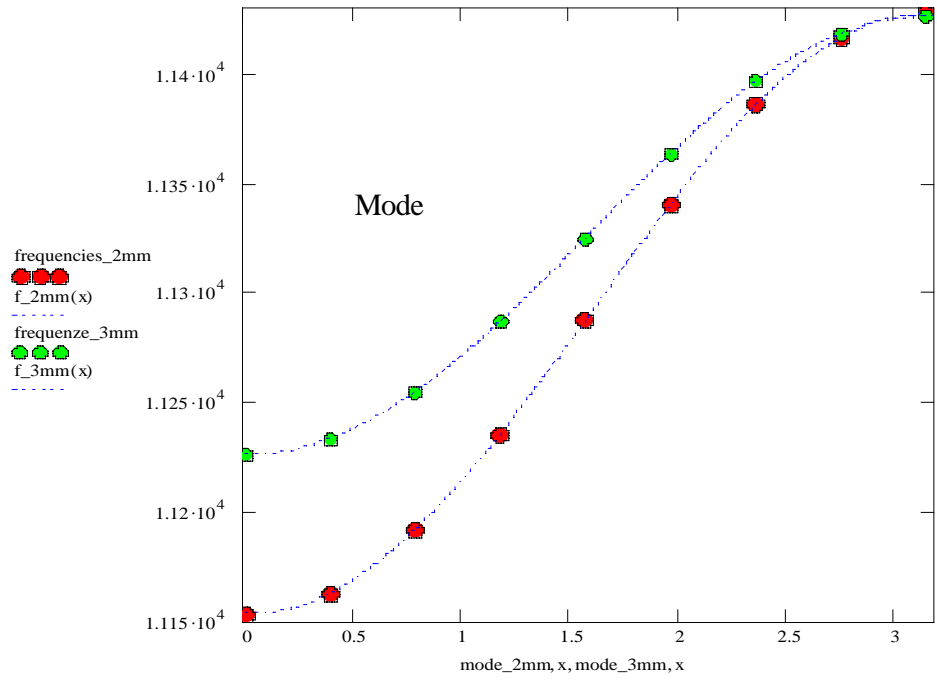


Fig. 4

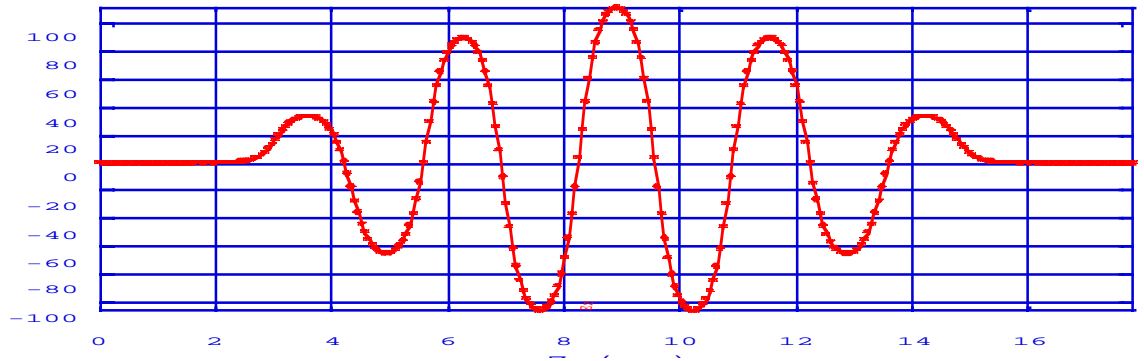


Fig. 5

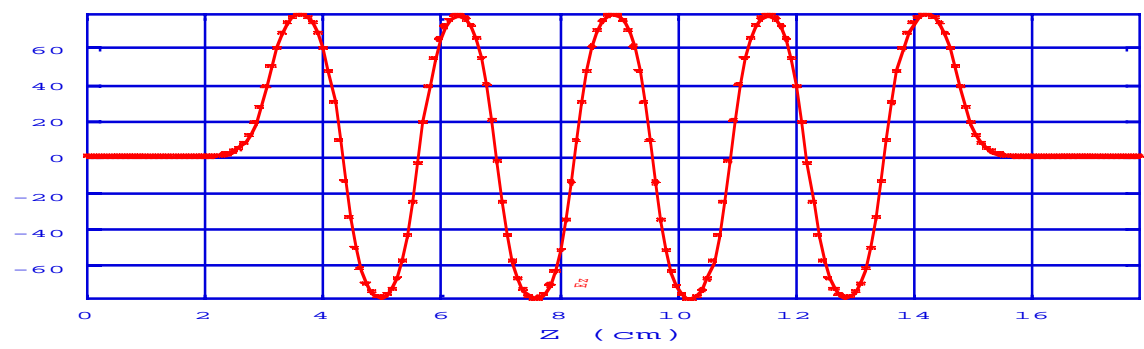


Fig. 6

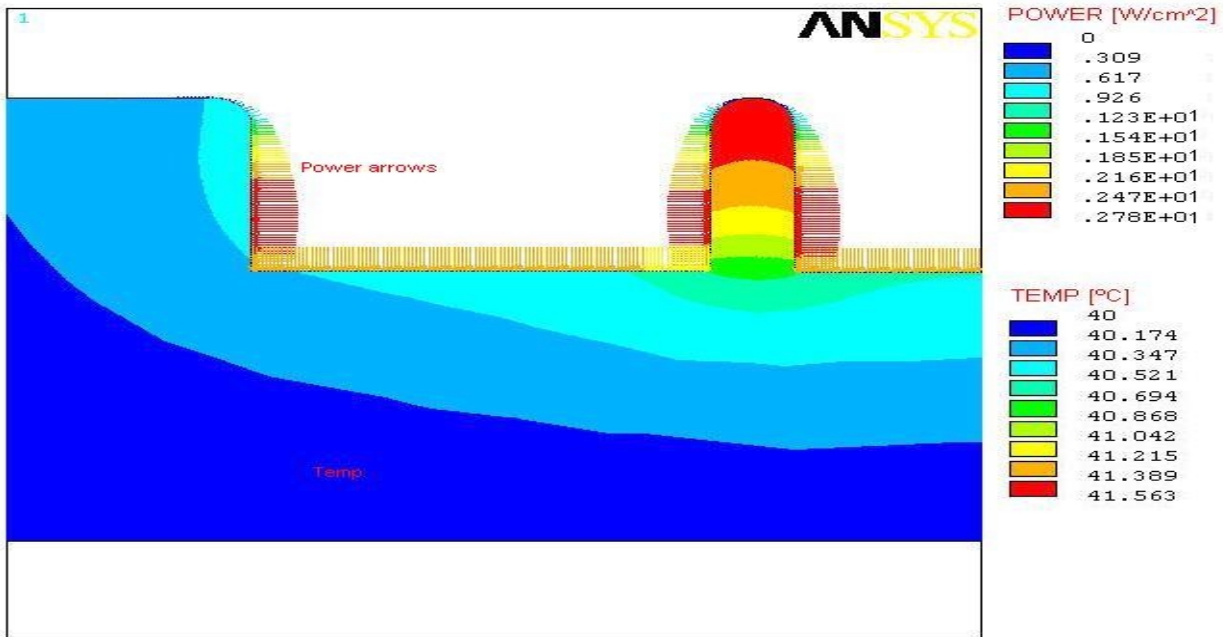


Fig. 7